nature neuroscience

Tanycytes of the hypothalamic median eminence form a diet-responsive neurogenic niche

Daniel A Lee[1,2], Joseph L Bedont[1,12], Thomas Pak[1,12], Hong Wang[1], Juan Song[2,3], Ana Miranda-Angulo[1,4], Vani Takiar[1], Vanessa Charubhumi[1], Francesca Balordi[5,6], Hirohide Takebayashi[7], Susan Aja[1,8], Eric Ford[9], Gordon Fishell[5,6] & Seth Blackshaw[1–3,10,11]

Adult hypothalamic neurogenesis has recently been reported, but the cell of origin and the function of these newborn neurons are unknown. Using genetic fate mapping, we found that median eminence tanycytes generate newborn neurons. Blocking this neurogenesis altered the weight and metabolic activity of adult mice. These findings reveal a previously unreported neurogenic niche in the mammalian hypothalamus with important implications for metabolism.

Several recent studies have reported neurogenesis in postnatal and adult mammalian hypothalamus[1–3]. The cell of origin and function of these newborn neurons, however, are unknown. Hypothalamic radial glia–like ependymal cells known as tanycytes are strong progenitor cell candidates that reside in the ventral hypothalamic ventricular zone[4]. Tanycytes are known to express neural stem cell markers such as Nestin[5]; previously, we found that tanycytes also express Notch pathway components and hypothalamic progenitor–specific transcription factors[6] such as Rax (**Supplementary Fig. 1**). Nonetheless, tanycytes have not previously been shown to proliferate substantially or to give rise to other cell types *in vivo*.

We quantified cell proliferation in mouse hypothalamus by conducting bromodeoxyuridine (BrdU) labeling in postnatal and adult mice. We observed substantial enrichment of BrdU$^+$ ependymal layer cells at the base of the third ventricle of the median eminence (MEm) relative to other hypothalamic regions (**Fig. 1a**,**b** and **Supplementary Fig. 2**). We named this proliferative domain the hypothalamic proliferative zone (HPZ) and determined by position, morphology and coexpression of the tanycyte markers[5] Nestin, Sox2 and vimentin that proliferating cells in this domain were β2-tanycytes (**Fig. 1c** and **Supplementary Fig. 2b–d**).

Concurrently, MEm neuronal numbers increased markedly from postnatal day 7 (P7) to P65, suggesting that HPZ cell proliferation reflects an active neurogenic zone (**Supplementary Fig. 3a**). To address this, we immunostained for BrdU and the pan-neuronal marker Hu and observed that 4.5 ± 1.1% of MEm Hu$^+$ neurons colabeled with BrdU, as compared with a much smaller fraction of Hu$^+$ BrdU$^+$ neurons in other hypothalamic regions (**Fig. 2** and **Supplementary Fig. 3b**). Furthermore, BrdU was coexpressed with other markers of mature hypothalamic neurons (**Supplementary Fig. 3c–g**). Fasting activates c-fos expression in ventrobasal hypothalamic neurons[7], and we observed Hu$^+$ BrdU$^+$ c-fos$^+$ MEm neurons (**Supplementary Fig. 4a**,**b**,**f**).

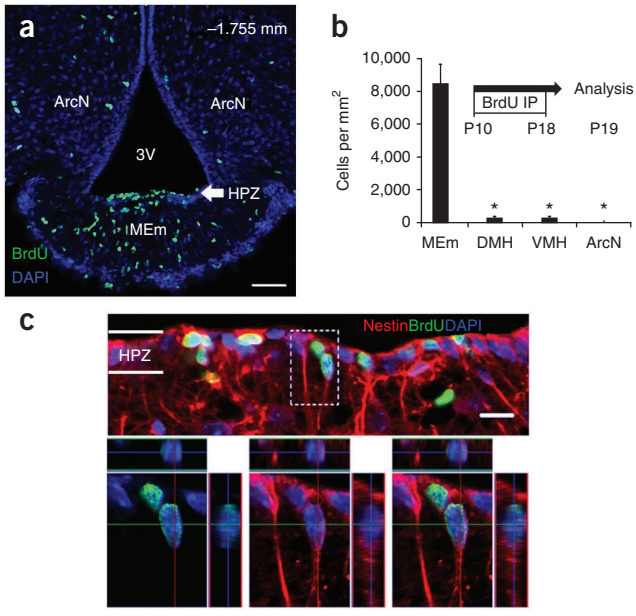

Figure 1 Hypothalamic proliferative zone. P19 mice received BrdU (P10–P18), and coronal ventrobasal hypothalamic sections were examined for BrdU immunostaining. (**a**) Hypothalamic proliferative zone (HPZ): enriched BrdU$^+$ cell population along the MEm ependymal layer of third ventricle (3V) floor. ArcN, arcuate nucleus. (**b**) Quantification of BrdU$^+$ ependymal layer cells juxtaposing hypothalamic nuclei ($n = 4$ mice; mean ± s.e.m.; $^*P < 0.01$): MEm (8,488.5 ± 1,134.8 cells/mm^2), ArcN (66.5 ± 54.0 cells/mm^2), ventromedial nucleus (VMH; 298.1 ± 58.3 cells/mm^2) and dorsomedial nucleus (DMH; 307.6 ± 90.3 cells/mm^2). (**c**) HPZ BrdU$^+$ cells are β2-tanycytes, with ependymal layer position, radial glial–like morphology and coexpression of tanycyte-enriched markers such as Nestin. Dashed box, higher-magnification *z*-stack reconstruction. Sections counterstained with DAPI (blue), a nuclear marker. Scale bars: 50 μm (**a**), 10 μm (**c**).

[1]Solomon H. Snyder Department of Neuroscience, Johns Hopkins University School of Medicine, Baltimore, Maryland, USA. [2]Institute for Cell Engineering, Johns Hopkins University School of Medicine, Baltimore, Maryland, USA. [3]Department of Neurology, Johns Hopkins University School of Medicine, Baltimore, Maryland, USA. [4]Universidad de Antioquia, Medellin, Colombia. [5]Neuroscience Program, Smilow Research Center, New York University School of Medicine, New York, New York, USA. [6]Department of Cell Biology, Smilow Research Center, New York University School of Medicine, New York, New York, USA. [7]Division of Neurobiology and Anatomy, Graduate School of Medical and Dental Sciences, Niigata University, Niigata, Japan. [8]Center for Metabolism and Obesity Research, Johns Hopkins University School of Medicine, Baltimore, Maryland, USA. [9]Department of Radiation Oncology, Johns Hopkins University School of Medicine, Baltimore, Maryland, USA. [10]Department of Ophthalmology, Johns Hopkins University School of Medicine, Baltimore, Maryland, USA. [11]Center for High-Throughput Biology, Johns Hopkins University School of Medicine, Baltimore, Maryland, USA. [12]These authors contributed equally to this work. Correspondence should be addressed to S.B. (sblack@jhmi.edu).

Received 21 November 2011; accepted 1 March 2012; published online 25 March 2012; doi:10.1038/nn.3079

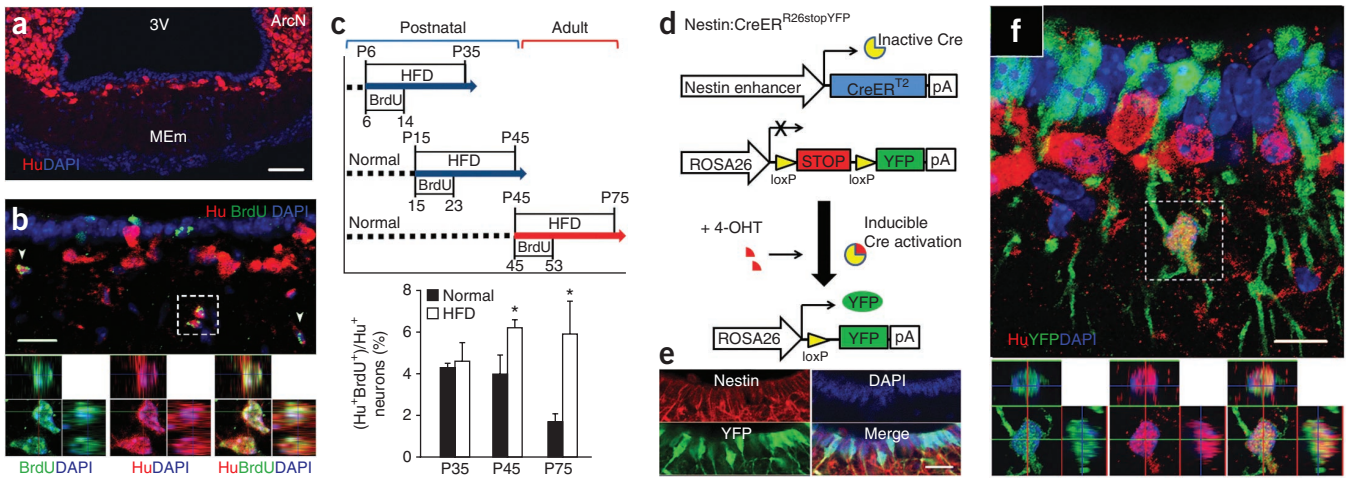

Figure 2 The median eminence is a neurogenic niche. (**a**) MEm neuronal distribution in P35 mice. (**b**) P35 mice received BrdU (P10–P18); MEm was immunostained for BrdU and the pan-neuronal marker Hu. Hu^+BrdU^+ coexpression is seen adjacent to the HPZ. (**c**) Age- and diet-dependent effects of MEm neurogenesis. Diagram of food and BrdU administration; mice are either fed normal chow entirely or switched to HFD. Newborn Hu^+BrdU^+ MEm neurons were quantified 1 month after BrdU administration ($n = 4$ mice; mean ± s.e.m.; $^*P < 0.05$). (**d**) Inducible transgenic approach used to fate map hypothalamic tanycytes. Nestin:$CreER^{R26stopYFP}$ mice permanently label tanycytes and their progeny with yellow fluorescent protein (YFP) after 4-hydroxytamoxifen (4-OHT) induction. (**e**) P7 Nestin:$CreER^{R26stopYFP}$ mice treated with 4-OHT 72 h earlier demonstrate specificity of tanycytic labeling via coexpression of YFP and $Nestin^+$ tanycytes. (**f**) P35 Nestin:$CreER^{R26stopYFP}$ mice were induced with 4-OHT at P4. Hu^+YFP^+ neurons present 1 month after induction, but not after a 72-h interval (**Supplementary Fig. 5g**). Sections were counterstained with DAPI (blue), a nuclear marker. Scale bars: 50 μm (**a**), 20 μm (**b**,**e**), 10 μm (**f**).

Similarly, leptin injection activates STAT3 in hypothalamic neurons[8], and 21.2 ± 4.2% (72 of 366 total counts for $n = 4$ mice) of newborn Hu^+ $BrdU^+$ neurons expressed phosphorylated STAT3 in leptin-injected BrdU-treated mice, as compared with 3.4 ± 1.7% (8 of 244 total counts for $n = 3$ mice) for fasted control mice (**Supplementary Fig. 4c–e**). These data suggest that newborn MEm neurons are functionally active.

Numerous studies have shown that a high-fat diet (HFD) during adolescent periods can lead to long-term food intake and weight changes[9]. To determine whether these changes correlated with hypothalamic neurogenesis, we conducted daily BrdU labeling at P6–P14, P15–P23 or P45–P53 in mice fed either normal chow or HFD ($P = 0.67$), examining mice 1 month after the initial BrdU injection (P35, P45 or P75, respectively; **Fig. 2c**). We observed no significant difference in neurogenesis between P35 mice fed normal chow or HFD; however, neurogenesis rates quadrupled in adult (P75) mice that were fed HFD compared with controls, with BrdU colabeling reaching 5.9 ± 1.6% of Hu^+ MEm neurons (114 of 1,941 total neurons for $n = 4$ mice; **Fig. 2c** and **Supplementary Table 1**). Thus, prolonged dietary changes can substantially affect HPZ neurogenesis into adulthood.

To address whether β2-tanycytes directly give rise to neurons *in vivo*, we bred transgenic Nestin:$CreER^{T2}$ driver mice[10] with ROSA26stopYFP reporter mice[11] to inducibly and selectively fate-map tanycytes and their progeny (**Fig. 2d–f**). Nestin:$CreER^{R26stopYFP}$ mice did not express yellow fluorescent protein (YFP) in ventral hypothalamus without administration of 4-hydroxytamoxifen (4-OHT; **Supplementary Fig. 5a**,**b**). Immediately after induction by 4-OHT at P4, $Nestin^+$ tanycytes were permanently labeled with YFP (**Fig. 2e**);

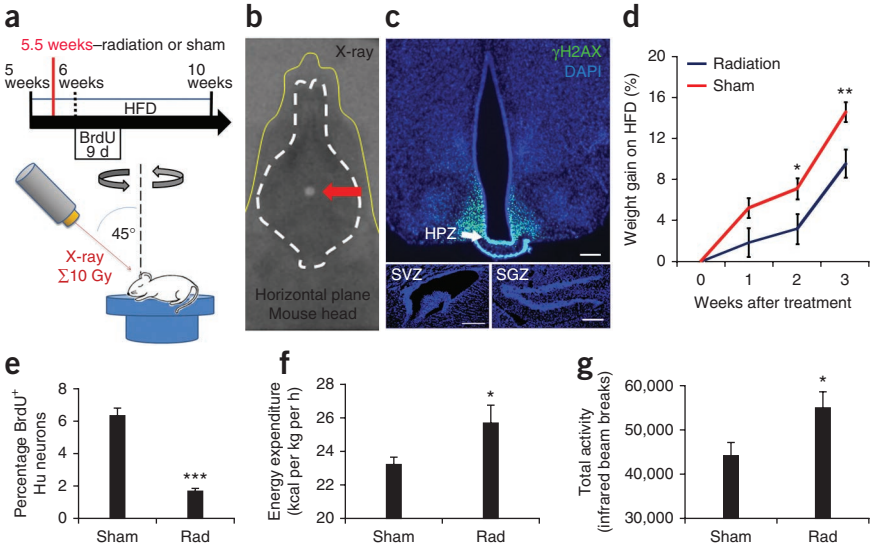

Figure 3 Median eminence neurogenesis regulates metabolism. (**a**) Experimental diagram of CT-guided irradiation of HPZ. (**b**) Superimposition of dosimetry-film acquired with 1-mm radiation beam in phantom with an X-ray of a real mouse subject (yellow line). White circle (arrow) indicates 10-Gy radiation dose focally targeted to HPZ. (**c**) Radiation targeting accuracy confirmed by γH2AX immunostaining, an indicator of radiation dose. γH2AX immunostaining is limited to the HPZ within the ventrobasal hypothalamus. SVZ, subventricular zone; SGZ, subgranular zone. Scale bars, 200 μm. (**d**) Attenuated weight gain in HFD-fed irradiated mice compared with parallel sham controls ($n = 9$). (**e**) MEm neurogenesis in irradiated versus sham-irradiated mice ($n = 4$ mice). (**f**) Higher energy expenditure observed in irradiated mice ($n = 11$). (**g**) Higher total activity observed in irradiated mice ($n = 11$). Mean ± s.e.m.; $^*P < 0.05$, $^{**}P < 0.01$; $^{***}P < 0.01$.

17.9 ± 1.7% (1,457 of 7,949 total cells for $n = 3$ mice) of $Sox2^+$ β2-tanycytes were labeled (**Supplementary Fig. 5c–e**). Notably, we observed no colabeling of YFP and the astrocyte marker glial fibrillary acidic protein or Hu immediately after induction (**Supplementary Fig. 5f,g**). At P35, 1 month after induction, a substantial fraction of Hu^+ MEm neurons were labeled with YFP (7.8 ± 0.6%, 160 of 2,097 total neurons for $n = 4$ mice; **Fig. 2f** and **Supplementary Fig. 5i**), suggesting that β2-tanycytes directly give rise to neurons *in vivo*. When P35 Nestin:$CreER^{R26stopYFP}$ mice were fasted, Hu^+ YFP^+ c-fos^+ MEm neurons were detected (**Supplementary Fig. 5h**), suggesting that newborn neurons are functionally active. We also observed a much smaller fraction of Hu^+ YFP^+ neurons in hypothalamic regions outside the MEm, with the MEm showing 43-fold higher neurogenesis than the arcuate nucleus after correction for the percentage of tanycytes labeled by the Nestin:$CreER^{T2}$ driver (**Supplementary Table 2**). Parallel negative-control experiments that prospectively labeled $Olig2^+$ oligodendrocyte precursor cells[12] suggested that they were not an appreciable source of newborn neurons (**Supplementary Fig. 6**). Taken together, these data suggest that β2-tanycytes are highly neurogenic.

We next probed the functional role of adult-born MEm neurons, using focal computed tomography (CT)-guided irradiation[13] to selectively inhibit adult MEm neurogenesis while sparing other neurogenic regions (**Fig. 3** and **Supplementary Fig. 7a–c**). Targeting of ventrobasal hypothalamus was guided by iodine-contrast CT scans and confirmed by X-ray dosimetry film (**Fig. 3b** and **Supplementary Fig. 7b**). Immunostaining for γH2AX, a sensitive readout of double-stranded DNA breaks that correlates strongly with radiation dosage[14], indicated that ventrobasal hypothalamus was targeted while other neurogenic niches were spared (**Fig. 3c**). Irradiated HFD-fed adult mice showed ~85% inhibition of MEm neurogenesis compared with sham-treated controls (**Fig. 3e**). Unexpectedly, HFD-fed adults gained significantly less weight and fat mass when irradiated than did sham controls (**Fig. 3d** and **Supplementary Fig. 7d,e**). Furthermore, oxygen consumption, energy expenditure and total activity were significantly elevated by irradiation of ventrobasal hypothalamus (**Fig. 3f,g** and **Supplementary Fig. 7f,g**). Taken together, these data suggest that adult MEm neurogenesis has a functional role in weight regulation.

In this study, we observed that levels of neurogenesis in MEm were more than fivefold higher than in other hypothalamic regions, and that newborn neurons are derived from β2-tanycytes. The potential physiological importance of this tanycyte neural progenitor pool is magnified by its position outside the blood-brain barrier and innervation by neurosecretory cells. Changes in the number and connectivity of MEm neurons may thus have an impact disproportionate to their number. Although we observe low levels of neurogenesis in other hypothalamic regions, lineage analysis shows that very few of these cells are derived from $Nestin^+$ tanycytes. These data also suggest that other as-yet-unidentified non-tanycyte progenitor cell populations may exist in postnatal hypothalamus.

Postnatal MEm neurogenesis is substantially enhanced by HFD and may lead to long-term changes in feeding and metabolism. HFD activation of MEm neurogenesis continues into adulthood, raising the possibility that this process might modulate hypothalamic neural circuitry late in life. Previous studies have shown that whole-brain X-irradiation leads to long-lasting changes in body weight[15]. We find that selectively inhibiting adult neurogenesis in the ventrobasal hypothalamus of HFD-fed animals leads to attenuated weight gain and higher levels of activity relative to controls. This suggests that MEm neurogenesis induced by overfeeding reduces baseline energy consumption and promotes energy storage in the form of fat. Such a response is likely adaptive in wild animals, for which rich food sources are rare, but maladaptive in laboratory housed mice. These findings raise the question of whether other dietary cues can regulate MEm neurogenesis, and whether this effect is observed in humans.

METHODS

Methods and any associated references are available in the online version of the paper at http://www.nature.com/natureneuroscience/.

Note: Supplementary information is available on the Nature Neuroscience website.

ACKNOWLEDGMENTS

We thank J. Nathans, S. Hattar, N. Gaiano, P. Achanta, C. Montojo, D. McClellan, T. Shimogori, T. Moran, E. Newman, M. Taylor and W. Yap for comments on the manuscript. We also thank M. Bonaguidi, C. Montojo, J. Reyes, M. Armour, E. Velarde, N. Forbes-McBean, W.F. Han and the Johns Hopkins School of Medicine Microscope Facility for technical advice and assistance. This work was supported by US National Institutes of Health grant F31 NS063550 and an NSF Graduate Fellowship (to D.A.L.), a Basil O'Connor Starter Scholar Award and grants from the Klingenstein Fund and NARSAD (to S.B.). S.B. is a W.M. Keck Distinguished Young Scholar in Medical Research.

AUTHOR CONTRIBUTIONS

D.A.L. and S.B. designed experiments. D.A.L., J.L.B., T.P., V.T., J.S., H.W., A.M.A., E.F., V.C. and S.A. performed experiments. D.A.L., J.L.B., T.P., A.M.A., V.C., S.A. and S.B. analyzed data. F.B., H.T. and G.F. contributed transgenic mice. D.A.L. and S.B. wrote the manuscript.

COMPETING FINANCIAL INTERESTS

The authors declare no competing financial interests.

Published online at http://www.nature.com/natureneuroscience/.
Reprints and permissions information is available online at http://www.nature.com/reprints/index.html.

1. Kokoeva, M.V., Yin, H. & Flier, J.S. *Science* **310**, 679–683 (2005).
2. Pierce, A.A. & Xu, A.W. *J. Neurosci.* **30**, 723–730 (2010).
3. Xu, Y. *et al. Exp. Neurol.* **192**, 251–264 (2005).
4. Mathew, T.C. *Anat. Histol. Embryol.* **37**, 9–18 (2008).
5. Rodríguez, E.M. *et al. Int. Rev. Cytol.* **247**, 89–164 (2005).
6. Shimogori, T. *et al. Nat. Neurosci.* **13**, 767–775 (2010).
7. Miller, I., Ronnett, G.V., Moran, T.H. & Aja, S. *Neuroreport* **15**, 925–929 (2004).
8. Cowley, M.A. *et al. Nature* **411**, 480–484 (2001).
9. Simerly, R.B. *Physiol. Behav.* **94**, 79–89 (2008).
10. Balordi, F. & Fishell, G. *J. Neurosci.* **27**, 14248–14259 (2007).
11. Srinivas, S. *et al. BMC Dev. Biol.* **1**, 4 (2001).
12. Masahira, N. *et al. Dev. Biol.* **293**, 358–369 (2006).
13. Ford, E.C. *et al. Radiat. Res.* **175**, 774–783 (2011).
14. Matinfar, M. *et al. Med. Image Comput. Comput. Assist. Interv.* **10**, 926–934 (2007).
15. D'Avella, D. *et al. J. Neurosurg.* **81**, 774–779 (1994).

ONLINE METHODS

Animals. Five-week-old or pregnant female C57BL/6 mice were obtained from Charles River Labs and housed in a 14-h/10-h light-dark cycle with free access to chow (Teklad F6 Rodent Diet 8664, Harlan Teklad, Madison, WI) and water. Where indicated, animals were provided with a high-fat diet (HFD) (60% of the calories as fat; Rodent Diet cat. no. D12492i, Research Diets, New Brunswick, NJ) *ad libitum* from P5–P35. Before weaning, this diet was supplied to nursing mothers. Normal chow and HFD administration for age- and diet-dependent effect experiment is outlined in **Figure 2c**. All mice used in these studies were maintained and euthanized according to protocols approved by the Institutional Animal Care and Use Committee at the Johns Hopkins School of Medicine.

Inducible Cre lines and mouse breeding. Nestin:CreER^{T2} mice, a generous gift of G. Fishell (New York University), were genotyped as previously described[10]. These mice were backcrossed for at least six generations into C57BL/6 strain and then crossed to the ROSA26stopYFP reporter line (Jackson Laboratory, Bar Harbor, ME). Double-heterozygous P4.5 pups (3–3.4 g body weight) received 0.2 mg 4-hydroxytamoxifen (4-OHT). Olig2:CreER mice, a generous gift of H. Takebayashi (Niigata University, Kumamoto, Japan), were crossed to the ROSA26stopYFP line. Double-heterozygous P4.5 pups received 0.25 mg 4-OHT. A sham oil vehicle control was performed on both sets of mutant animals in parallel with 4-OHT induction experiments.

POMC:Cre mice[8] obtained were crossed to the Z/EG (C57BL/6 background) reporter line (both from Jackson Laboratory; Bar Harbor, ME). Double-heterozygous pups received BrdU pulses on P10–P18 as indicated below.

Reagents. *Bromodeoxyuridine (BrdU) and 4-hydroxytamoxifen (4-OHT).* Where indicated, animals received bromodeoxyuridine (BrdU; Sigma) administrated in the morning and evening by intraperitoneal (i.p.) injection at 50 mg/kg of body weight from P10 to P18. For examination of temporal changes in median eminence (MEm) neurogenesis (**Fig. 2c**), mice were administered BrdU by i.p. injection for 9 d for the dates indicated. For BrdU saturation studies examining proliferative changes in the HPZ over time (**Supplementary Fig. 2f**), 50 mg/kg of BrdU was administered by i.p. every 2 h for 12 h. Mice were subsequently sacrificed at the end of this 12-h period. 4-Hydroxytamoxifen (4-OHT) (Sigma, St. Louis, MO) was prepared as a 50 mg/ml stock solution in anhydrous ethanol. 4-OHT was sonicated in a heated water bath, and 100 µl of dissolved solution was pipetted into 500 µl of corn oil (Sigma, St. Louis, MO), and vortexed. Ethanol was evaporated off by heated vacuum centrifuge. The 4-OHT/oil solution was administered to mice by oral gavage.

Tissue processing and antibodies. Postnatal and adult mice were sacrificed, perfused with 2% or 4% paraformaldehyde in PBS, and cryoprotected as previously described[10]. Serial sections (40 µm thick) were collected and stored at −20 °C. Free-floating sections were immunostained using the following primary antibodies and working concentrations: sheep polyclonal anti-BrdU (1:500; AB1893, Abcam, Cambridge, MA), rat monoclonal anti-BrdU (1:200; BU1/75, Accurate, Westbury, NY), rabbit polyclonal anti-Sox2 (1:1,500; AB5603, Chemicon, Temecula, CA), mouse monoclonal anti-Nestin (1:100; Rat-401, BD Pharmingen), mouse monoclonal anti-vimentin (1:100; 40E-C, DSHB), mouse monoclonal anti-Hu (5 µg/ml; 16A11, Molecular Probes, Carlsbad, CA), mouse monoclonal anti-GFAP (1:500; MAB360, Chemicon, Temecula, CA), rabbit polyclonal anti-GFAP (1:500; Z033429, DAKO), rabbit polyclonal anti-Olig2 (1:500; AB15328, Chemicon, Temecula, CA), rabbit polyclonal anti-NG2 (1:500; generous gift from B. Stallcup, Sanford-Burnham Medical Research Institute, La Jolla, CA, USA), goat polyclonal anti-Dcx (1:200; sc-8066, Santa Cruz, Santa Cruz, CA), rabbit polyclonal anti-pSTAT3 (1:2,000; 9131, Cell Signaling, Beverly, MA), rabbit polyclonal anti-GFP (1:1,000; A-11122, Invitrogen), chicken polyclonal anti-GFP (1:500, Aves Lab, Oregon), mouse monoclonal anti-GAD6 (1:200; GAD-6, DSHB), rabbit polyclonal anti-MAP2 (1:50; HPA008273, Sigma) and rabbit polyclonal anti-c-fos (1:500; sc-52, Santa Cruz). Double and triple staining was visualized with Alexa Fluor 488–, Alexa Fluor 555–, Alexa Fluor 568–, Alexa Fluor 594– or Alexa Fluor 633–conjugated secondary antibodies (1:500, Molecular Probe, Carlsbad, CA). 4′,6-Diamidino-2-phenylindole (DAPI) was used as a nuclear counterstain, unless otherwise noted.

Immunohistochemistry and *in situ* hybridization. For BrdU immunostaining, sections were first incubated in 2 N HCl at 37 °C for 30 min and then rinsed in 0.1 M boric acid (pH 8.5) at room temperature for 10 min. Sections were next rinsed in PBST (PBS + 0.01% Triton X-100) blocked for 5 min in SuperBlock (ScyTek) and incubated overnight with in anti-BrdU antibody in 5% normal horse serum in PBS/0.16% Triton X-100 blocking solution at 4 °C. Sections were washed in PBST, incubated with secondary antibodies in blocking solution at RT for 2 h, washed in PBST, mounted on Superfrost Plus slides (Fisher), and coverslipped with Gelvatol mounting medium. *In situ* hybridization techniques and sequences of probes (i.e. NPY) used, have been previously described[6].

Cell quantification. All tissue sections used for quantification were imaged using confocal microscopy (Meta 510, Zeiss Microscopy). MEm cells were counted. The dorsal-ventral boundary of the cells counted was the third ventricle floor and the ventral edge of the external layer of the MEm. The lateral boundaries were a 20-µm medial inset off the corner of the third ventricle. In only one instance (**Supplementary Fig. 4**, Hu$^+$pSTAT3$^+$BrdU$^+$ counts), the lateral boundaries were set at the corners of the median eminence. MEm dorsal and ventral boundaries remained identical to those previously described. For examination of the number of proliferative cells within the ependymal layer, BrdU$^+$ cells in the ependymal layer of the third-ventricle floor (coronal section) were counted. Seven 40-µm coronal serial sections (280 µm) were counted between −1.515 mm and −1.875 mm from bregma. On the rare occasion, a section would be lost in the collection process; in such instances the next adjacent section in the mouse sample was taken and counted (seven sections were counted total). For analysis of newborn Hu$^+$ neurons, for each section analyzed, Hu$^+$DAPI$^+$ and Hu$^+$BrdU$^+$DAPI$^+$ neurons within the MEm were counted in the region defined above, excluding cells of the uppermost focal plane to avoid oversampling. To determine the frequency of BrdU$^+$ cells expressing Hu, dual fluorescence–labeled sections were examined by confocal microscopy using a 20× objective and 1.5× digital zoom. For each marker and treatment condition, seven representative serial sections from each of four animals were examined. Sections were scored for double or triple labeling by manual examination of optical slices. Cells were considered positive for a given phenotypic marker when the marker-specific labeling was unambiguously associated with a BrdU$^+$ nucleus. Cells were spot-checked in all three dimensions by *z* stack using a 63× objective. Images of Hu$^+$BrdU$^+$DAPI$^+$ labeling in feeding conditions (**Fig. 2** and **Supplementary Fig. 4**) were blinded before counting. Cells were corrected for number of optical slices and overcounting of large neurons with Abercrombie correction[16]. Cell counts are described in the text and figure legends as mean of several samples ± s.e.m., total cell counts, and the number of samples examined to derive those total cell counts.

Quantitative magnetic resonance spectroscopy and *in vivo* metabolic analysis. Female C57BL/6J mice maintained on HFD beginning at 5 weeks underwent irradiation ($n = 9$) or sham procedure ($n = 9$) at 5.5 weeks of age. At 10 weeks, mice were placed in the EchoMRI-100 (Echo Medical Systems) scanner, which allows for the measurement of whole-body fat mass, lean tissue mass, free water and total body water in live animals with quantitative magnetic resonance spectroscopy.

A different cohort of female C57BL/6J mice maintained on HFD beginning at 4.5 weeks underwent irradiation ($n = 11$) or sham procedure ($n = 12$) at 5.5 weeks of age. Two weeks after treatment, mice were then tested in a Comprehensive Lab Animal Monitoring System (CLAMS, Columbus Instruments) for simultaneous measurements of powdered high-fat diet intake, physical activity (infrared beam breaks) and whole-body metabolic profile by indirect calorimetry. After several days of acclimation, mice were monitored as follows: rates of oxygen consumption (VO_2, ml/kg/h) and carbon dioxide production (VCO_2) were measured for each chamber every 24 min throughout the study; respiratory exchange ratio (RER = VCO_2 / VO_2) was calculated by Oxymax software (v. 4.70) to estimate relative oxidation of carbohydrate (RER = 1.0) versus fat (RER approaching 0.7), not accounting for protein oxidation; and rates of energy expenditure were calculated as EE = $VO_2 \times (3.815 + (1.232 \times \text{RER}))$[17] and normalized for subject body mass (kcal/kg/hr). Average metabolic values were calculated per subject and averaged across subjects for statistical analyses by paired, two-tailed test (unequal variance) for the last day in the metabolic chamber (dark portion of day), when mice were most acclimated for metabolic testing.

Focal irradiation of ventrobasal hypothalamus. Radiation (10 Gy) was delivered using the Small Animal Radiation Research Platform (SARRP), a dedicated laboratory radiation device developed in house[13]. Each mouse was anesthetized

using ketamine and placed on the robotically controlled stage of the SARRP unit. A computed tomography (CT) image was acquired with the SARRP (voxel size 0.2 mm), and the third ventricle was identified on this scan. To confirm target visualization, a CT image was acquired on mice using iodine contrast injected intrathecally, which allows the ventricles to be directly visualized on CT images ($n = 3$)[13]. From the dual iodine-contrast CT analysis, an anatomical template was used for all following irradiation targeting of the median eminence. After the target was identified on CT, the mouse was moved under robotic control to align this target with the radiation delivery beam of the SARRP. Using a 1-mm-diameter beam collimator, an arc technique was used to deliver 10 Gy to the target point[14]. Previous measurements indicate that this technique provides very low doses of radiation (<0.1 Gy) outside the 1-mm target. The area of the pituitary gland and surrounded structures is therefore effectively shielded from irradiation. The accuracy of the beam targeting has been measured in previous studies to be within 0.2 mm both in phantom tests[14] and in tissue sections[13]. As further confirmation for the present study, we performed immunohistochemical staining on three mice, 1 h after irradiation, against γH2Ax, the well-known histone protein that is an early marker of DNA double-strand breaks[13]. This provides direct visualization of the areas of tissue affected by the radiation beam.

Sham controls were performed in parallel. Mice in this cohort were caged, transported to the procedure room, and received the same anesthesia and similar amounts of ambient radiation coming from the SARRP as the irradiated cohort. Sham controls differed only in that they did not receive a direct radiation beam.

Statistical analysis. Figures are shown as mean ± s.e.m. The Student's *t*-test was used and, where needed, was corrected for unequal variance or was corrected for multiple comparisons by using the Dunn-Šidák correction.

16. Abercrombie, M. *Anat. Rec.* **94**, 239–247 (1946).
17. Lusk, G. *The Elements of the Science of Nutrition* 4th edn. (W.B. Saunders, Philadelphia, 1928).

doi:10.1038/nn.3079